Science of the Total Environment 921 (2024) 170958

Contents lists available at ScienceDirect

Science of the Total Environment

journal homepage: www.elsevier.com/locate/scitotenv

Soil temperature and moisture as key controls of phosphorus export in mountain watersheds

Gordon Gianniny [a,*], John M. Stark [b], Benjamin W. Abbott [c], Raymond Lee [c], Janice Brahney [a]

[a] Department of Watershed Sciences, Utah State University, Old Main Hill, Logan, UT 84322, United States of America
[b] Department of Biology, Utah State University, Old Main Hill, Logan, UT 84322, United States of America
[c] Department of Plant & Wildlife Sciences, Brigham Young University, Provo, UT, United States of America

HIGHLIGHTS

- Soil temperature increases water-soluble phosphorus (P) export from mountain soils.
- Low soil moisture limits the effects of warming on P export and soil respiration.
- Warming-driven increases in P are most likely when soil moisture is also elevated.
- Soil warming may impair mountain water quality by increasing soil P export.

GRAPHICAL ABSTRACT

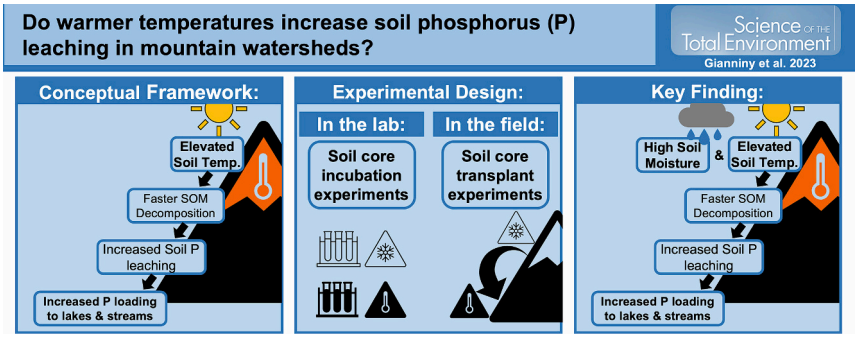

ARTICLE INFO

Editor: Ouyang Wei

Keywords:
Phosphorus
Mountain lakes
Soil warming
Nutrient cycling
Eutrophication

ABSTRACT

Oligotrophic mountain lakes act as sensitive indicators of landscape-scale changes in mountain regions due to their low nutrient concentration and remote, relatively undisturbed watersheds. Recent research shows that phosphorus (P) concentrations are increasing in mountain lakes around the world, creating more mesotrophic states and altering lake ecosystem structure and function. The relative importance of atmospheric deposition and climate-driven changes to local biogeochemistry in driving these shifts is not well established. In this study, we test whether increasing temperatures in watershed soils may be contributing to the observed increases in mountain lake P loading. Specifically, we test whether higher soil temperatures increase P mobilization from mountain soils by accelerating the rate of geochemical weathering and soil organic matter decomposition. We used paired soil incubation (lab) and soil transplant (field) experiments with mountain soils from around the western United States to test the effects of warming on rain-leachable P concentration, soil P mobilization, and soil respiration. Our results show that while higher temperature can increase soil P mobilization, low soil moisture can limit the effects of warming in some situations. Soils with lower bulk densities, higher pH, lower aluminum oxide contents, and lower ratios of carbon to nitrogen had much higher rain-leachable P concentration across all sites and experimental treatments. Together, these results suggest that mountain watersheds with high-P soils and relatively high soil moisture could have the largest increases in P mobilization with warming.

Abbreviations: Ptase, phosphatase enzyme; pNP, *p*-nitrophenyl phosphate; LOI, loss on ignition; LMM, linear mixed model; SOM, soil organic matter; TP, total dissolved phosphorus; TOC, total organic carbon; TN, total nitrogen.

* Corresponding author at: 753 Clement St., South Lake Tahoe, CA 96150, United States of America.
E-mail address: ggianniny@gmail.com (G. Gianniny).

https://doi.org/10.1016/j.scitotenv.2024.170958
Received 23 October 2023; Received in revised form 11 February 2024; Accepted 11 February 2024
Available online 14 February 2024

Consequently, lakes and streams in such watersheds could become especially susceptible to soil-driven eutrophication as temperatures rise.

1. Introduction

As air temperature continues to rise across the world (USGCRP, 2018), mountain lakes can act as sensitive indicators of otherwise hard to detect landscape-scale changes in mountain regions. Mountain lakes are typically oligotrophic, so even small changes in processes that affect nutrient and solute delivery can have profound effects on mountain lake water chemistry and ecology (Moser et al., 2019). Recent research has identified one such trend in mountain lakes around the world: increasing phosphorus (P) concentration (e.g. Kopàček et al., 2011; Stoddard et al., 2016). Notably, P increases are present even in remote, relatively undisturbed mountain watersheds, ruling out many of the traditional point and nonpoint sources often responsible for P pollution in water bodies (Stoddard et al., 2016).

Increasing P concentration in mountain lakes are of concern for multiple reasons. Many mountain lakes are P-limited, likely due to historically elevated atmospheric nitrogen (N) deposition (Goldman, 1988; Camarero and Catalan, 2012). As a result, mountain lake primary productivity and community structure are and will likely continue to be sensitive to even relatively small increases in P. This dynamic is already playing out in mountain lakes across the world, many of which have undergone a P-driven shift from oligotrophic to mesotrophic regimes (Morales-Baquero et al., 2006; Brahney et al., 2014; Oleksy et al., 2020; Davidson et al., 2023). In general, P-driven eutrophication results in decreased lake ecosystem biodiversity, simplified phytoplankton and macrophyte community structure, and overall ecosystem instability (Qin et al., 2013). Changes in mountain lake water chemistry are usually driven by changes in the airsheds and watersheds around those lakes (Moser et al., 2019), so the observed increases in mountain lake P-loading imply that P loading is increasing across entire mountain landscapes. Landscape-scale P increases in mountainous regions could alter nutrient limitation status of these ecosystems and, in some cases, increase or decrease soil carbon (C) sequestration by impacting primary productivity and organic matter decomposition (Shaw and Cleveland, 2020). In extreme cases, these changes could also degrade water quality in the mountain watersheds that provide a water source for >1.5 billion people around the world (Mu et al., 2020).

Identifying the cause of elevated P delivery to mountain lakes is the first step in mitigating and managing the impacts of higher P availability in mountain ecosystems. Several hypotheses have been put forward to explain the observed P increases, including recovery from acidification (e.g., Kopáček et al., 2019; Scholz and Brahney, 2022), increased dust-mediated atmospheric P deposition (Morales-Baquero et al., 2006; Brahney et al., 2015), and increasing wildfire activity (e.g Olson et al., 2023). While all of these mechanisms likely play a role for some lakes, they fall short of explaining P increases in mountain watersheds with no history of acid deposition, no nearby dust source, and no recent wildfire activity. In light of this discrepancy, Scholz and Brahney (2022) proposed a fourth possible explanation of widespread increases in mountain lake P concentration: Higher soil temperature drives faster soil organic matter (SOM) decomposition and geochemical weathering, which increases P export from mountain soils into streams and lakes.

Warming-driven soil P mobilization has a strong theoretical basis, and recent soil incubation studies lend further support to this hypothesis. Phosphorus enters the labile soil pool through two primary mechanisms: geochemical weathering and SOM decomposition (Weintraub, 2011). Both mechanisms are temperature sensitive (Conant et al., 2011; Brantley et al., 2023) and are hypothesized to proceed faster at higher temperatures (Brantley et al., 2023; Arroyo et al., 2022; Wallenstein et al., 2010). Taken together, faster geochemical weathering and faster SOM decomposition in warmer conditions could substantially increase water-soluble soil P concentrations and, by extension, P export from soils into mountain lakes and streams.

In addition to this robust theoretical basis, there is preliminary evidence from lab incubation and plot-scale studies that warming can increase soil P availability (Shaw and Cleveland, 2020) and leaching (Scholz and Brahney, 2022; Kaštovská et al., 2022). However, it remains unclear how these findings apply to the wide range of soil types and climatic regimes present in mountain regions. In this study, we seek to address this knowledge gap by testing how environmentally relevant levels of soil warming affect mountain soil P mobilization under typical field conditions. We addressed this question through two complementary approaches. First, we conducted lab incubation experiments with mountain soils collected along elevation gradients in five US mountain ranges across a variety of latitudes and bedrock geologies. This experiment tested whether the findings of other incubation experiments could be replicated under more "field-like" soil moisture and temperature conditions. Second, we conducted year-long reciprocal soil core transplant experiments in two of these mountain ranges. Transplant experiments are often used to simulate environmental changes by transplanting soils along temperature, precipitation, or other climatic gradients (e.g., Powers, 1990; Link et al., 2003; Waring and Hawkes, 2018). Here, we took advantage of the natural temperature gradient present in most mountain systems by transplanting cores from higher/cooler elevations to lower/warmer elevations to simulate the effects of climate change in a field setting. The purpose of this experiment was to provide insight into the effects of warming on soil P mobilization over longer timescales under real-world conditions. We hypothesized that higher soil temperatures would increase soil organic matter decomposition rates, leading to higher levels of rain-soluble and bioavailable soil P. We expected this effect to be most pronounced in soils with low aluminum (Al) and iron (Fe) oxide contents, a pH around 6–7, and high SOM contents, as soils with these characteristics generally have larger labile P pools (Kruse et al., 2015).

2. Methods

2.1. Lab incubation experiments

2.1.1. Site description & sampling design

We collected intact soil cores in five different mountain ranges (Fig. 1) with varying climates and bedrock geologies: the Brooks Range (Alaska), Bear River (Utah), San Juan (Colorado), Sierra Nevada (California), and Uinta Mountains (Utah). These mountain ranges cover a broad range of parent materials, parent material P concentration, soil types, vegetation types, and climates (Table S1). In the Bear River, San Juan, and Uinta mountains, we collected samples at approximately 300 m intervals from the bottom of the foothills to the highest accessible elevation. In the Sierra Nevada, the uppermost elevation was set by a wilderness boundary, and samples were collected at 300 m intervals from that elevation downwards.

Initially, sites were selected in south-facing (aspect between 135 and 225°) meadows or clearings with slope angles under 20° using ArcGIS and CalTopo. Some sites had to be relocated to locations falling outside these criteria due to access and/or sampling issues at the initially selected sites. The final aspect, slope, and vegetation characteristics of each site are given in Table S2. Samples from the Brooks Range were collected by a crew from the Toolik Field Station at four pre-existing sites between the coastal plain (at the northernmost extent) and the northern foothills of the mountain range. Because these sites were established for another project, they had more variable aspects, slopes, and vegetation types.

At each sampling site, we collected 12 soil cores of 10-cm depth and 5-cm diameter by pounding lengths of polycarbonate pipe into the soil surface. Vegetation was cleared from the soil surface prior to sampling, but the entire top 10 cm of the soil was collected, including O horizons when present. We collected centric systematic area samples by setting up a 4 m × 4 m grid with one corner on a pre-selected GPS point, then collecting cores from the center of each 1 m × 1 m grid cell. This approach ensured that core collection locations were evenly distributed over the sampling area to avoid the clumping that can occur with random area sampling (Krebs, 2013). Following sample collection, we stored intact cores on ice and shipped or transported them back to Utah State University (USU) within 48 h. Upon arrival at USU, three of the 12cores collected were randomly selected for soil property characterization, while the remainder of the samples were randomly assigned to one of three incubation treatments. Because soil microbial biomass has been shown to decrease with time in refrigerated storage (Stenberg et al., 1998) and cores from different mountain ranges had differing amounts of storage time between collection and incubation, all cores were stored frozen at approximately −20°C until analysis or incubation. Freezing does affect soil biota, but these effects are consistent regardless of storage time and tend to be small in soils that frequently undergo freeze-thaw cycles in the field (Stenberg et al., 1998).

2.1.2. Experimental design

Soils were incubated in three temperature treatment regimes ($n = 3$ cores from each site in each treatment) using growing chambers (CONVIRON Model A1000, Controlled Environments Inc., Pembina, ND). We determined the incubation treatment temperature regimes using the average air temperatures from SNOTEL stations in three different elevation classes (<2740 m, 2740–3100 m, and >3100 m) in three study mountain ranges (Bear River, San Juan, and Uinta). For each station, we calculated mean minimum and maximum temperature for each week of the growing season (defined by the USDA as soil temperatures > 5°C at a depth of 5 cm). We used these weekly mean minimum and maximum temperature as the minimum and maximum temperature for each day of our incubation treatments, such that temperature during one day of the incubation fluctuated from the average minimum to the average maximum air temperature during the corresponding week of the growing season. Because our growing chambers had a minimum set point of 5°C, we selected the subset of days with minimum temperatures > 5°C from our simulated growing seasons to be used for incubation treatments. The highest elevation class had the shortest period with minimum temperatures > 5°C (10 days), so we set the length of our incubations to 10 days. Cores were also subjected to diurnal light fluctuations, with the day/night length for each day determined by calculating the average day length during the corresponding week of the year at the average latitude of the four study mountain ranges in the contiguous US (40°). We added a two-day thawing period at a constant temperature at the beginning of each incubation run in order to allow for microbial recovery after frozen storage as suggested by Stenberg et al. (1998). We selected this more complex incubation regime rather than using three constant temperatures because many soil microbes are only active in specific temperature ranges and light conditions (Koch et al., 2007), some of which would be missed by using constant temperature incubations. The resulting incubation treatments are available in Table S3.

Incubations were conducted over three successive runs in the three different growing chambers such that each treatment was repeated once in each chamber, with one core from each source site incubated in each chamber during each run. This design allows replication within each treatment without confounding treatment and chamber effects. Before starting each incubation run, cores were weighed and placed in 1-L mason jars. Cores were incubated at ambient moisture content (i.e., the moisture content present when collected) in an effort to mimic field conditions. Mason jars were loosely capped using lids with scintillation valves to minimize water loss during incubation. Soil respiration samples were collected on days five and ten of each incubation (Table 2). On the day before each measurement, jars were flushed with lab air, then

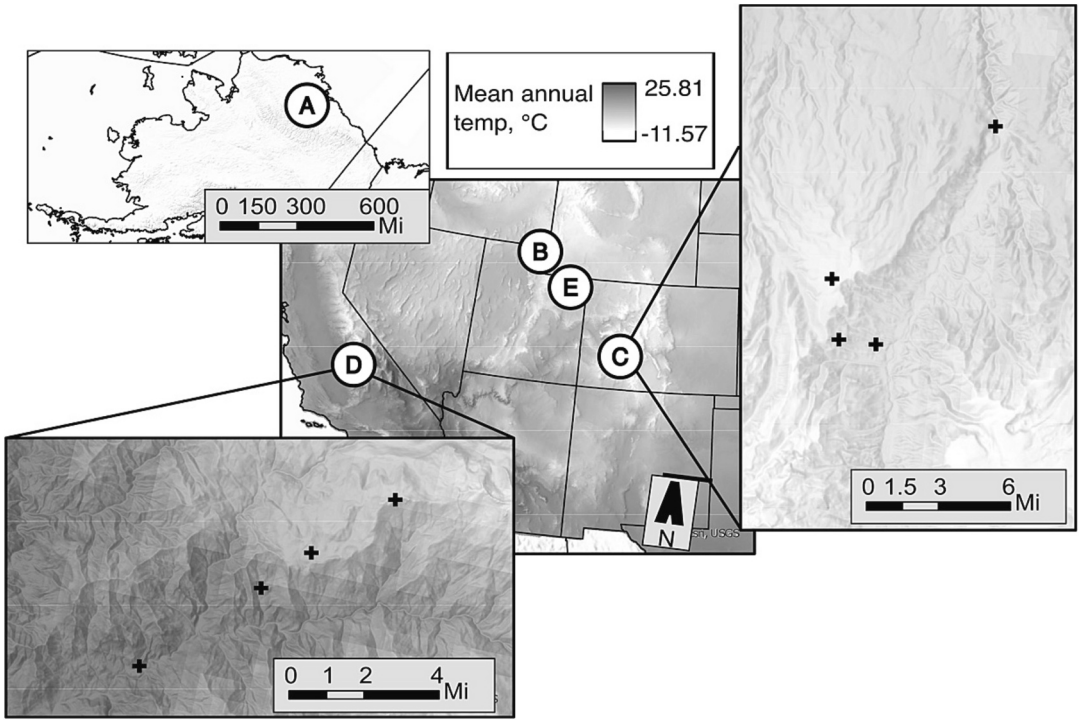

Fig. 1. Site overview map showing the approximate locations and mean annual temperatures of sample collection sites in the Brooks Range (A), Bear River Range (B), San Juan Mountains (C), Sierra Nevada (D), and Uinta Mountains (E). Expanded views of the San Juan and Sierra Nevada mountains show the locations of the four sites used for transplant experiments in each range (marked by black plus signs). Temperature data was obtained from the PRISM Climate Group's 30-year normals dataset (Copyright © 2022, PRISM Climate Group, Oregon State University, https://prism.oregonstate.edu. Map created 12/29/2022).

sealed for 24 h. After 24 h, gas samples were collected through the scintillation valves in the jar lids using a gas-tight syringe. Samples were stored in exetainer vials and analyzed for CO_2 concentration on a Shimadzu GC-2014 (Shimadzu Scientific, Columbia, MD). At the end of each incubation run, cores were re-weighed to estimate water loss during incubation, then emptied into sample bags. Samples were again stored frozen until analysis to account for differences in storage time between incubation and analysis, as samples could only be processed 15–20 at a time.

2.1.3. Soil respiration calculations

CO_2 concentration in soil respiration samples were measured using a Shimadzu GC-2014 (Shimadzu Scientific, Columbia, MD). Soil respiration rates, in terms of $\mu g\ CO_2\ g\ dry\ soil^{-1}\ hour^{-1}$, were calculated based on the CO_2 concentration in the headspace of the incubation jar, the mass of soil in the jar, and the length of the incubation period. After measuring respiration rates at 5 and 10 days, we estimated the total CO_2 (μg per g soil) respired throughout the 10-day incubation using the following assumptions: (1) the first respiration measurement is a rough approximation of average soil respiration rates over the first five days of the incubation, and (2) the second respiration measurement is a rough approximation of average soil respiration rates over the second five days of the incubation. Total soil respiration was then calculated by taking the mean of the two respiration measurements. This calculation likely produced underestimates of actual total soil respiration due to the exponential decline in respiration that usually occurs following thaw (e.g Schimel and Clein, 1996). However, this approach still allows for comparisons between total respiration values for different samples because the bias towards underestimating respiration is consistent across all samples.

2.1.4. Soil nutrient analyses

After the incubation experiments, we estimated rain-soluble phosphorus (P), carbon (C), and nitrogen (N) in each soil core by extracting samples with a dilute salt "synthetic rain" solution. It should be noted that after our synthetic rain extraction, we analyzed nutrient concentration in each sample following protocols for water samples. As a result, while we report "total" P, C, and N values for our samples, these results reflect the total concentration of each nutrient extracted by our synthetic rain solution rather than the "total" amount of each nutrient in each soil. After thawing and sieving incubated samples, a 1 g subsample from each core was extracted using a synthetic rainwater solution with a pH of about 5.5 prepared following Grover et al. (2016; Table S5). Subsamples were extracted with 30 ml of synthetic rain and shaken for 16 h at 250 rpm on an orbital shaker. Samples were then centrifuged at 1800 rpm for 20 min, filtered to remove large particulates using 5.0 μm PTFE syringe filters, and frozen until analysis. Rain-soluble total dissolved phosphorus (hereafter "rain-soluble P") was measured by diluting and acidifying filtered samples, then analyzing P concentration on an Agilent 8900 ICP-MS Triple Quad (Agilent Technologies Inc., Santa Clara, CA) in the ICP MS Metals Laboratory at the University of Utah. Rain-soluble total organic carbon (rain-TOC) and total nitrogen (rain-TN) in each sample were measured using a Skalar Formacs-Series TOC and TN analyzer (Skalar Inc., Buford, GA).

2.2. Transplant experiments

2.2.1. Site descriptions & sampling design

We carried out reciprocal transplant experiments to test the effects of warming on soil P production in the Sierra Nevada (CA) and San Juan Mountains (CO) (Fig. 1). We selected these two mountain ranges for the transplant experiments because they had the largest elevation gradients of our five study mountain ranges and, by extension, the largest temperature gradients of the five ranges (Fig. 1). In addition, the Sierra Nevada and San Juan Mountains have contrasting bedrock geologies and climates (Table S1), allowing for a more robust investigation of the effects of warming on nutrient production under a variety of conditions. For each mountain range, we selected four soil core collection/incubation "gardens" that were approximately evenly distributed over the range of accessible elevations. As with the incubation soil collection sites, initial sites were located in south-facing (135–225° aspect) meadows or clearings with slope angles under 20°, but some sites had to be relocated due to sampling issues. The actual elevations, aspects, slopes, and vegetation types of the final sites are given in Table S4.

At each of these sites, we used a 4 m × 4 m centric grid to collect 15 intact soil cores by pounding 10-cm deep × 5-cm diameter polycarbonate pipe into the soil surface. When present, vegetation was cleared from the soil surface prior to sampling. Three cores from each site were randomly selected for soil property analyses and were transported on ice back to USU, where they were frozen at −2° C until analysis. The remaining 12 cores were randomly assigned to a transplant garden and stored on ice while being moved to their transplant site.

2.2.2. Transplant experimental design

We conducted a full reciprocal transplant experiment in each mountain range, meaning that cores from each source site were transplanted to each of the three other garden sites ($n = 3$ cores per source site in each transplant garden). In addition, three cores from each site were transplanted to different holes in the same site as a disturbance control. After transplanting between all four sites in each mountain range, this resulted in four transplant gardens, each with three cores from each source elevation. Prior to burying each core in its transplant garden, we attached a nylon bag containing 10 g (approximately 14.1 meq (−) charge per bag) of mixed-bed ion exchange resin beads (Amberlite MB-20H/OH form) to the base of each core to capture ion flux during the transplant period. Cores were collected and transplanted in June 2021 and left in place until June 2022. We monitored soil temperature and moisture conditions at a 5 cm depth in each transplant garden during the transplant period by installing Onset HOBO soil temperature and moisture data loggers (Onset Computer Corporation, Bourne, MA) at each site. After the first six months of the transplant period, we re-visited the San Juan sites and replaced the resin bead bags attached to each core with fresh bags to avoid exceeding the exchange capacity of the bags. Wildfires in the area around the sites in the Sierra Nevada prevented us from re-visiting the Sierra sites until the end of the transplant period in summer 2022.

2.2.3. Soil nutrient analyses

At the end of the year-long transplant period, we brought the cores back to the lab and analyzed rain-soluble nutrient concentrations, resin-captured nutrient concentrations, and Ptase enzyme activity in each core along with a suite of soil properties for each site. Rain-soluble nutrient measurements allowed us to estimate the effects of transplanting to different elevations on nutrients that could easily be leached into nearby waterbodies in a single storm, while resin-captured nutrients provide an approximation of total nutrient flux through the soil core during the transplant period, which could also ultimately reach nearby lakes and streams. Ptase activity is often used to infer the level of P limitation in soils because it is up-regulated when P availability is low (Wallenstein et al., 2010). In addition, we measured post-transplant soil wetness by drying subsamples of each soil core at 105 °C for 48 h. All analyses were carried out immediately following the end of the transplant period.

We followed the same synthetic rain extraction protocol described above to estimate rain soluble TOC, TN and TP. Samples were extracted within 48 h of collection, then rain-TOC and TN were measured using the Skalar-Formacs Series TOC/TN analyzer (Skalar Inc., Buford, GA). Rain-soluble P was measured using molybdate blue colorimetry (after Murphy and Riley, 1962) following a persulfate digestion (EPA method 365.3) on a SpectraMax M2e microplate reader (Molecular Devices, San Jose, CA).

We measured total P, ammonium (NH_4^+), and nitrate (NO_3^-) captured

by the resin bead bags by extracting the beads with 2 M potassium chloride (KCl). Resin bead bags were stored at 4 °C until extraction, then a 2-g sub sample of beads was shaken with 40 ml of 2 M KCl for 1 h at 250 rpm (after Noe, 2011). Resin bead total P (hereafter "resin-P") in the KCl extracts was measured using the molybdate blue method (Murphy and Riley, 1962) following a persulfate digestion (EPA method 365.3) as described above. In addition, NH_4^+ and NO_3^- in resin bead extracts were measured using the salicylate colorimetric method for NH_4^+ (Nelson, 1983) and salicylic acid nitration for NO_3^- (Cataldo et al., 1975).

Finally, acid and alkaline Ptase activity were measured by mixing subsamples of each soil with a *p*-nitrophenyl phosphate (pNP) substrate solution. Samples were mixed with buffer solutions at pH 6.5 and 11.0 for acid and alkaline Ptase, respectively (after Tabatabai, 1994), then incubated at room temperature with one mol of pNP substrate for 1 h. Next, 0.5 M sodium hydroxide (NaOH) was added to each sample to develop color by reacting with liberated *p*-nitrophenyl. The amount of *p*-nitrophenyl liberated by each soil was calculated by measuring each sample's absorbance at 410 nm on a SpectraMax M2e microplate reader (Molecular Devices, San Jose, CA). Final enzyme activities for each assay, in terms of μg P g dry soil^{-1}hour^{-1}, were calculated following Eq. (2.1):

$$Activity\left(\frac{\mu g\ P}{g\ dry\ soil \times hour}\right) = P_{\mu g} \times \frac{V_{extract}}{M_{soil} \times T_{assay}} \tag{2.1}$$

where: $P_{\mu g}$ is the measured P concentration in each sample (μg P/ml), $V_{extract}$ is the amount of buffer solution (ml) added to each soil, M_{soil} is the mass of dry soil (g) used for the assay, and T_{assay} is the total assay time (hours). We also calculated the total enzyme activity for each soil by adding the acid and alkaline Ptase activity for that sample.

2.3. Soil property analyses

In addition to nutrient analyses, we measured a suite of soil properties to identify the primary controls on rain-soluble soil P concentration across all sites. First, we estimated bulk density by dividing fine soil (<2 mm) volume by fine soil weight. Bulk density calculations were made assuming a rock fragment particle density of 2.65 g/cm^3 for the >2 mm soil fraction. Following bulk density estimation, samples were sieved to 2 mm and then used to measure loss on ignition (LOI), pH, extractable iron (Fe) and aluminum (Al), total carbon (TC), and total nitrogen (TN) content. While most of these analyses were carried out for all cores, more costly/time-consuming analyses (extractable Fe/Al, pH) were carried out on a subset of samples from each site ($n = 3$ per site). Soil moisture, SOM content, and carbonate content were determined by heating samples at 50 °C for 24 h, 500 °C for 4 h, and 1000 °C for 2 h respectively. In addition to this LOI procedure, core-level gravimetric soil moisture content was measured for each soil core after the incubation or transplant period by drying for 48 h at 105 °C. pH was measured in a 2:1 (by weight) deionized (DI) water to soil mixture using a Mettler-Toledo SevenExcellence pH probe (Mettler-Toledo LLC, Columbus, OH). Extractable Fe and Al were measured via extraction with two different solutions: sodium pyrophosphate to extract organic-associated Fe and Al, and sodium-citrate dithionite to extract organic-associated, amorphous, and oxide Fe and Al as described by Carter and Gregorich (2008). Extracts were analyzed on an Agilent 8900 ICP-MS Triple Quad (Agilent Technologies Inc., Santa Clara, CA) in the USU Geochemistry Lab. Amorphous and oxide Fe and Al concentrations for each soil were calculated by subtracting pyrophosphate extracted Fe/Al from citrate extracted Fe/Al for that soil. TC and TN were measured via combustion at 1000 °C on a Thermo Scientific Delta V Advantage IRMS (Thermo Fisher Scientific, Waltham, MA) in the USU Geochemistry Lab, and C:N ratios for each soil were calculated.

2.4. Statistical analyses

2.4.1. Incubation experiments

We used two statistical approaches to assess the effects of incubation treatment and soil moisture on rain-soluble P and total soil respiration rates. First, we used nested ANOVAs to test the effects of incubation treatment on rain-soluble P and total soil respiration within each mountain range. Next, we fit nested linear models to test the effects of core-level moisture content on rain-soluble P and total soil respiration within each mountain range. We also used nested linear models to examine correlations between rain-soluble P, rain-TOC, and rain-TN. These models took the general form:

$$(Y)_i = \beta_0 + \beta_1(SM_i, TOC_i, TN_i)/R_i \tag{2.2}$$

where Y_i is rain-soluble P or total soil respiration of the "i^{th}" core, SM_i is the soil moisture content of the "i^{th}" core, TOC_i is the rain-TOC concentration of the "i^{th}" core, TN_i is the rain-TN concentration of the "i^{th}" core, R_i is the source mountain range of the "i^{th}" core, and β_0 and β_1 are constants.

2.4.2. Transplant experiments

To assess the effects of year-long transplant on P availability in mountain soils, we used linear mixed models (LMMs) and regression tree (RT) analysis to model the relationship between each of our response variables (rain-soluble P, resin-P, and Ptase activity) and soil temperature and moisture data collected by the data loggers installed at each site. First, LMMs took the general form:

$$(Y)_i = \beta_0 + \beta_1 M_i + \beta_2 T_i + \beta_3 PTW_i + SS_i b_i \tag{2.3}$$

where: $(Y)_i$ is the rain-soluble P, resin-P, or Ptase activity of the "i^{th}" core, M_i is the average soil moisture content at the "i^{th}" core's transplant site, T_i is the average soil temperature at the "i^{th}" core's transplant site, PTW_i is the post-transplant wetness (g water per g dry soil) of the "i^{th}" core, SS_i is the "i^{th}" core's source site, and $\beta_0 \ldots \beta_3$ and b_i are constants. We treated transplant site soil temperature, transplant site soil moisture, and post-transplant wetness as fixed effects and fit a random intercept for source site to account for variation between soils from different source sites.

For each analysis, we used the average soil temperature and moisture conditions in each transplant site for the entire duration of the period that the analyte in question represented. Average soil temperature and moisture data were obtained from ONSET Hobo data loggers installed in each transplant site for the duration of the transplant period. Following this framework, we used average soil temperature and moisture across the entire duration of the transplant period for rain-soluble P in both mountain ranges and resin-P in the Sierra Nevada, as these analyses were carried out once at the end of the transplant period. For resin-P in the San Juans, we analyzed the first and second batches of resin beads separately. For the first set, which was in place from June 2021–October 2021, we used the average soil moisture and temperature conditions during that period. For the second set, which was in place from October 2021–June 2022, we used average soil moisture and temperature values during that time. This approach allowed us to capture seasonal changes in warming/P dynamics.

For each of these models, we tested variations of this model with all possible fixed effect combinations, and then selected the model with the lowest Akaike information criterion (AIC) from each season for use in final analyses. When multiple models had AIC scores within two units of each other, we reported the results of both models. We repeated this process separately for our two study mountain ranges, as initial data exploration suggested that the mountain ranges had markedly different responses. Models were fit using the lme4 package (Bates et al., 2014) in R (R Core Team, 2022). To assess the significance of predictor variables in our models, we used the Satterthwaithe method (Satterthwaite, 1941) to estimate degrees of freedom and calculate *P*-values using the lmerTest

package (Kuznetsova et al., 2017). We reported predictor variables with $P < 0.1$ as "marginally significant" and variables with $P < 0.05$ as "significant" due to the high variability inherent in most environmental data.

Second, we used regression tree models to test the effects of transplant site soil temperature and moisture on rain-soluble P and resin-P production. For these analyses, we calculated the difference in rain-soluble P and resin-P concentrations between control cores and cores transplanted to other sites in order to estimate changes in rain-soluble P and resin-P production caused by transplant. This "P difference" was calculated following Eq. (2.4):

$$P_{di} = P_{mi} - P_{ci} \tag{2.4}$$

where P_{di} is the rain-soluble P or resin-P difference for the "i^{th}" core used for regression tree analysis, P_{mi} is the measured rain-soluble P or resin-P

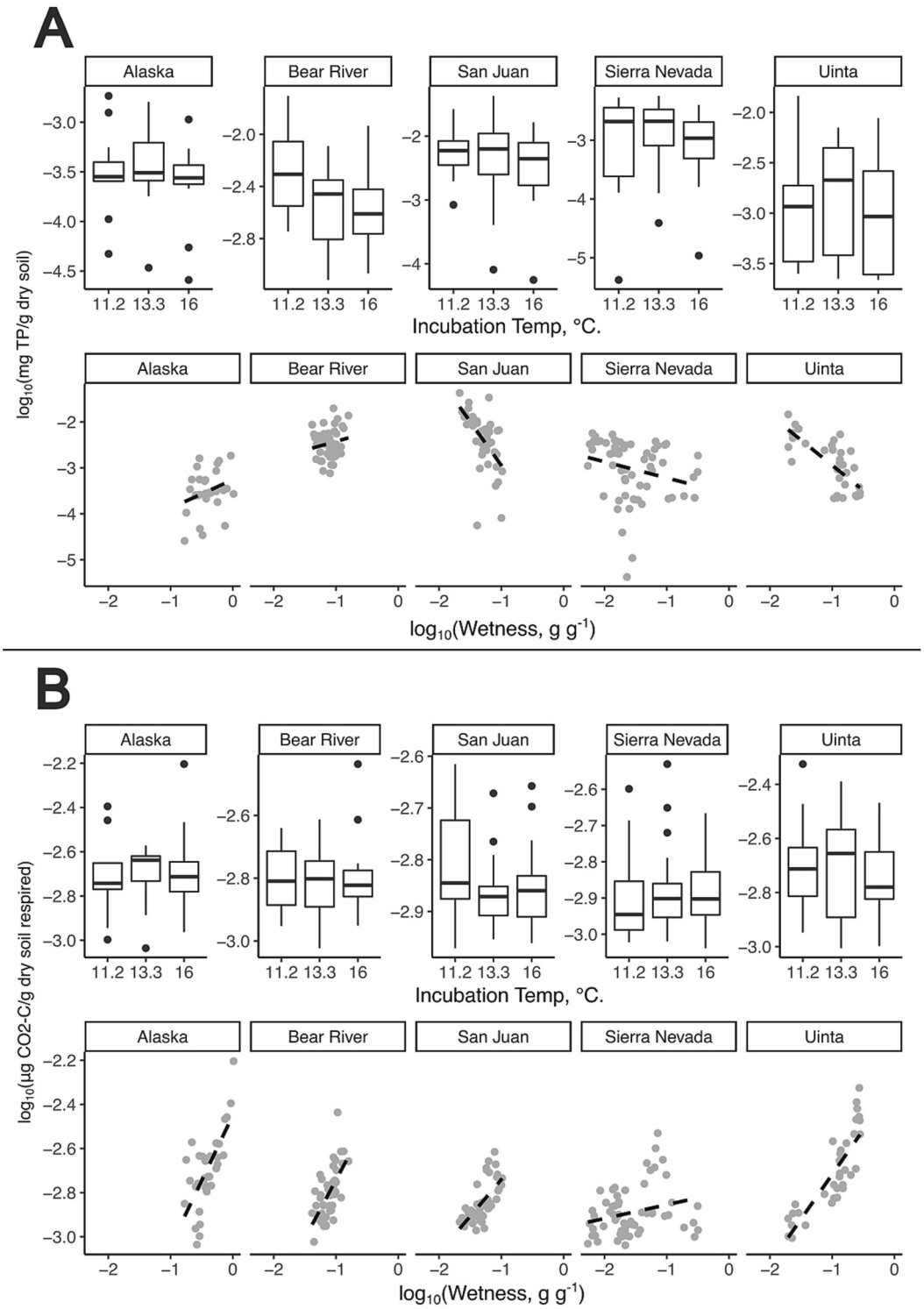

Fig. 2. Boxplots and scatterplots showing the effects of incubation temperature (top; nested ANOVA) and soil wetness (bottom; nested linear models) on rain-soluble P (A) and total soil respiration (B). Temperature had no significant effect on rain-soluble P or soil respiration in any mountain range, while soil wetness had a positive correlation with respiration in all five mountain ranges.

concentration for the "i^{th}" core, and P_{ci} is the mean rain-soluble P or resin-P concentration of disturbance control cores from the "i^{th}" core's source site. Regression tree models were fit for both rain-soluble P difference and resin-P difference using the rpart package (Therneau and Atkinson, 2022) in R (R Core Team, 2022) using mean annual transplant site soil temperature and moisture as predictor variables.

2.4.3. Soil properties

Regression tree modeling was used to test which soil properties played significant roles in determining rain-soluble P across all sites. Regression tree models testing the effects of all soil properties (bulk density, pH, soil moisture, organic content, carbonate content, TC/TN, C:N ratio, and Fe/Al content) on rain-soluble P were fit using the rpart package (Therneau and Atkinson, 2022) in R (R Core Team, 2022). Variable importance for each soil property was calculated using the caret package (Kuhn, 2015). We used rain-soluble P as our response variable for soil property modeling because rain-soluble P data were available for both our incubation and transplant samples.

3. Results

3.1. Lab incubation experiments

We observed no effect of soil temperature on soil P production (Fig. 2A) or on soil respiration (Fig. 2B) across temperature regimes. Instead, soil moisture was the primary driver of soil respiration across all study sites. Nested ANOVAs and Tukey post-hoc testing showed that while average rain-soluble P concentration varied between different mountain ranges ($F(4, 208) = 29.11, P < 0.01$), incubation temperature had no effect on rain-soluble P within each mountain range ($F(10, 208) = 0.61, P = 0.81$). Tukey HSD post-hoc testing showed that Soils from the Bear River and San Juan Mountains had significantly higher rain-soluble P concentration ($\overline{x} = 4.5$ & 7.7 μg P/g dry soil) than those from the Brooks, Sierra Nevada, and Uinta Mountains ($\overline{x} = 0.46$, 1.8, & 2.3 μg P/g dry soil; $P < 0.01$)

Total soil respiration also varied among mountain ranges but was unaffected by temperature. Soils from the Brooks Range and Uinta Mountains had significantly higher total soil respiration than soils from the Bear River, San Juan, or Sierra Nevada Mountains ($F(4, 208) = 17.40, P < 0.01$; Fig. 2B). As with rain-soluble P, incubation temperature had no significant effect on total soil respiration within each mountain range ($F(10, 208) = 0.35, P = 0.97$).

While temperature had no effect on rain-soluble P or total soil respiration, both variables were significantly correlated with soil wetness. Overall, a nested linear model of the form $[(Rain - soluble\ P)_i = \beta_0 + \beta_1(Wetness_i)/Range_i]$ was statistically significant $(R^2 = 0.49, F(9, 213) = 22.35, P < 0.01)$.The model showed that soil wetness was not correlated with rain-soluble P in soils from the Brooks ($\beta = 0.62, P = 0.15$) or Bear River mountains ($\beta = 0.39, P = 0.47$), possibly because the narrow ranges of soil wetness present in these mountain ranges limited the significance of correlations between wetness and rain-soluble P. In contrast, soil moisture had a significant negative correlation with rain-soluble P in soils from the San Juan ($\beta = -1.91, P < 0.01$), Sierra Nevada ($\beta = -0.35, P = 0.01$), and Uinta Mountains ($\beta = -1.10, P < 0.01$) (Table S6).

Correlations between soil wetness and total soil respiration were more consistent across all study mountain ranges. Overall, a nested linear model of the form $[(Total\ soil\ respiration)_i = \beta_0 + \beta_1(Wetness_i)/Range_i]$ was statistically significant $(R^2 = 0.59, F(9, 213) = 33.51, P < 0.01)$.Wetness had a significant positive correlation with total soil respiration in the Brooks ($\beta = 0.59, P < 0.01$), Bear River ($\beta = 0.53, P < 0.01$), San Juan ($\beta = 0.33, P < 0.01$), Sierra Nevada ($\beta = 0.06, P = 0.03$), and Uinta Mountains ($\beta = 0.40, P < 0.01$) (Table S7). Correlations between rain-soluble P and total soil respiration were not consistent across ranges. The overall model of the form $[(Rain - soluble\ P)_i = \beta_0 + \beta_1(Total\ soil\ respiration_i)/Range_i]$ was statistically significant $(R^2 = 0.46, F(9, 213) = 20.7, P < 0.01)$.Rain-soluble P and respiration were not correlated in the Brooks and Bear River Ranges, but total soil respiration had a significant negative correlation with rain-soluble P in the San Juan ($\beta = -2.96, P < 0.01$) and Uinta Mountains ($\beta = -1.82, P < 0.01$) and a positive correlation with rain-soluble P in the Sierra Nevada ($\beta = 2.24, P < 0.01$).

Rain-soluble P concentrations were also strongly linked with rain-TOC concentration in all but one of the five study mountain ranges. The overall nested linear model of the form $[(Rain - TP)_i = \beta_0 + \beta_1(Rain - TOC_i)/Range_i]$ was statistically significant $(R^2 = 0.43, F(9, 194) = 33.53, P < 0.01)$. Rain-TOC had a strong positive correlation with rain-soluble P in soils from the San Juan ($\beta = 1.59, P < 0.01$), Sierra Nevada ($\beta = 0.89, P < 0.01$), and Uinta mountains ($\beta = 0.47\ P < 0.01$) and a marginally significant positive correlation with rain-soluble P in soils from the Brooks Range ($\beta = 0.36, P = 0.08$). Rain-TOC and Rain-soluble P were not significantly correlated in the Bear River mountain range ($\beta = -0.06, P = 0.78$). Rain-TN concentrations were below the limit of detection for most samples, so correlations between rain-TN and rain-soluble P could not be estimated.

Overall, model fit for nested linear models was mediocre, with R^2 values ranging from 0.43 to 0.59. While these models explain relatively low proportions of overall variance in the data, the amount of data available for each treatment condition was insufficient to support more complex multivariate models that may have explained higher proportions of variance. Incorporating additional environmental data such as soil properties would likely have improved model fit, but we lacked enough statistical power to do so in a robust manner. With this in mind, we feel that the results presented above warrant further discussion in spite of the relatively low proportion of variance explained by these models.

3.2. Transplant experiments

Transplant experiment results showed substantial differences in soil nutrient responses to seasonal patterns in temperature and moisture in the two study mountain ranges. The data logger at the second-lowest site in the Sierra Nevada was damaged by wildlife shortly after deployment, rendering its soil temperature and moisture data unusable. Data from the remaining loggers show that summer soil temperature generally decreased while soil moisture increased with increasing elevation in both mountain ranges. One-way ANOVAs and Tukey post-hoc tests showed that during the summer, all sites in the Sierra Nevada were significantly warmer than any site in the San Juan Mountains ($F(1, 2260) = 859.8, P < 0.01$), while all sites in the San Juans were significantly wetter than any site in the Sierra Nevada ($F(1, 2260) = 1956.6, P < 0.01$). These patterns generally persisted into the fall. In the winter, all sites in the Sierra Nevada remained significantly warmer than any San Juan site ($F(1, 2260) = 566.98, P < 0.01$). However, unlike the summer, all Sierra Nevada sites were significantly wetter than all but the wettest San Juan site ($F(1, 2260) =, P < 0.01$). Additionally, while the trend of lower temperature at higher elevation persisted in the Sierra Nevada during the winter, a temperature inversion formed in the San Juan Mountains. All sites in the San Juans also had average soil temperatures below 0 °C during the winter, while all Sierra Nevada sites remained well above freezing. On average, the second highest site was the warmest during the winter in the San Juans, while the lowest elevation site was the coldest.

The distinct climates in the Sierra Nevada and San Juans drove different seasonal changes in rain-soluble P, resin-P flux, and Ptase activity between the two mountain ranges. In the San Juans, rain-soluble P and Ptase activity were correlated with soil temperatures near the end of the transplant period. For the first batch of resin bead bags (June–Oct), resin-P had a marginally significant positive correlation with June–Oct. average soil temperature ($P = 0.06$; Table 1). During this period, both

soil temperature and moisture were elevated (Fig. 3). For the second batch of resin beads (Oct–June), resin-P was positively correlated with Oct.–June average soil moisture ($P = 0.02$; Table 1). Soil temperatures were below 0 °C for much of this period. Linear mixed models combining transplant affect variables showed that the only significant predictor of rain-soluble P was a log transform of post-transplant soil wetness ($P < 0.01$), which had a strong negative correlation with soil temperature over the last 50 days of the transplant period (hereafter "50-day temperature"). With this relationship in mind, we also tested LMMs modeling the effects of 50-day temperature on rain-soluble P, which found a strong positive correlation between rain-soluble P and 50-day temperature (Fig. 3, Table 1). Similarly, post-transplant soil moisture was the only significant predictor of acid, alkaline, and total Ptase activity in the San Juans. Sites with higher post-transplant soil moisture had significantly higher Ptase activity than those with lower post-transplant soil moisture (Fig. 3, Table 1).

Unlike rain-soluble P and Ptase activity, resin-P was not correlated with post-transplant wetness or soil temperature conditions over the last 50-days of the transplant period. Instead, LMMs showed that Jun.–Oct. temperature was the only significant predictor of resin-P for the first batch of resin bead bags (Fig. 3, Table 1), while Oct.–Jun. moisture was the only significant predictor of resin-P for the second batch of bags (Table 1).

In the Sierra Nevada, both rain-soluble P and resin-P had negative correlations with annual average soil moisture and positive correlations with annual average soil temperature, while Ptase activity was not correlated with any transplant effect variable. Most samples from the two highest elevation sites had very low rain-soluble P concentration (at or below the limit of detection). While this affected the ability to detect changes in rain-soluble P in soils from these sites, LMM results show that annual soil moisture had a marginally significant negative effect on rain-soluble P ($P = 0.08$), while annual soil temperature had a marginally significant ($P = 0.10$) positive effect on rain-soluble P (Fig. 4; Table 2).

Similarly, resin-P was positively correlated with annual temperature and negatively correlated with annual soil moisture in the Sierra Nevada (Table 2; Fig. 4). Notably, soil temperature and moisture were closely linked in the Sierra Nevada ($R^2 = 0.96, P < 0.01$), so it is unclear which variable is driving the observed responses in rain-soluble P and resin-P from a statistical perspective. Unlike rain-soluble P and resin-P, Ptase activity was unaffected by soil temperatures in the Sierra Nevada. Neither total, acid, nor alkaline Ptase activity were correlated with any soil climate variable, possibly because of the narrow range of Ptase activities present in the Sierra Nevada (Table 2).

Across both mountain ranges, regression tree models showed that transplant site soil moisture and temperature both affected rain-soluble P and resin-P differences. Regression tree models showed that increases in rain-soluble P occurred only in the soil cores transplanted to sites with average annual soil temperatures $> 10^{\circ}$C and soil moisture contents $\geq 0.16\ m^3/m^3$ (Fig. 5A). Notably, transplant site temperature was a better candidate for the root node split than transplant moisture, suggesting that temperature exerts a stronger control on rain-soluble P difference than moisture. In contrast, transplant moisture was a better candidate for the root node split in modeling resin-P difference (Fig. 5B), suggesting that transplant moisture content exerts a stronger control on resin-P difference than temperature. Increases in resin-P occurred either when soil moisture was $\geq 0.25\ m^3/m^3$ or when soil moisture was $< 0.25\ m^3/m^3$ and transplant site soil temperature was $\geq 12^{\circ}$C.

While the two mountain ranges had different patterns of rain-soluble P, resin-P, and Ptase activity, rain-soluble P and rain-TOC were significantly correlated in both mountain ranges. Linear models showed that rain-soluble P was positively correlated with rain-TOC in both the San Juans $(R^2 = 0.36, P < 0.01)$ and the Sierra Nevada $(R^2 = 0.16, P < 0.01)$. As with samples from the lab incubation experiments, rain-TN concentration were below the limit of detection for most samples, so the relationship between rain-soluble P and rain-TN could not be estimated.

3.3. Soil property effects

Across all samples from the Brooks, Bear River, San Juan, Sierra Nevada, and Uinta mountains, the soils with alkaline pH's, lower aluminum oxide concentration, and higher carbonate contents had higher rain-soluble P concentration. Regression tree modeling showed that bulk density was the most important predictor of rain-soluble P, followed by Al oxide content, C:N ratio, carbonate content, Fe oxide content, soil pH, soil moisture, and SOM content (Fig. 6). Of these variables, a regression tree using pH as the primary root node, Al oxide content and bulk density as second-tier internal nodes, and then C:N ratio and carbonate content as subsequent internal nodes produced the lowest RMSE (0.00496; Fig. 6). Finally, a lower C:N ratio was associated with higher soil P concentration across all study mountain ranges. Soils with pH ≥7, Al oxide concentration < 2 %, and carbonate content ≥ 2.1 % were predicted to have an average rain-soluble P concentration an

Table 1
Descriptive statistics for Linear Mixed Models (LMMs) testing soil climate effects on rain-soluble total dissolved phosphorus (rain-TP), phosphatase enzyme (ptase) activity, and resin-bead total phosphorus (resin-TP) in the San Juan mountains. Predictor variables included post-transplant wetness, soil temperature over the last 50 days of the transplant period ("50 day temp."), summer soil temperature and moisture (June–Oct. soil temp/moisture), and winter soil temperature and moisture (Oct.–June soil temp/moisture).

Rain-TP					
Model	AIC	β	df_{Sat}	T	P_{Sat}
log_{10}(rain TP) ~ log_{10}(post − transplant wetness)	39.90	−0.52	43.27	−3.96	<0.01
log_{10}(rain TP) ~ 50 day Temp.	34.90	0.03	31.01	3.198	<0.01

Ptase activity					
Model	AIC	β	df_{Sat}	T	P_{Sat}
log_{10}(total Ptase activity) ~ log_{10}(post − transplant wetness)	28.64	0.40	43.26	3.32	<0.01
log_{10}(total Ptase activity) ~ 50 day Temp.	24.94	−0.02	31.01	−2.28	0.03

Resin-TP					
Model	AIC	β	df_{Sat}	T	P_{Sat}
log_{10}(Jun − Oct Resin TP) ~ June − Oct soil temp.	56.17	0.03	42.05	1.93	0.06
log_{10}(Oct − Jun Resin TP) ~ Oct − June soil moisture	111.36	5.02	45.42	2.25	0.02

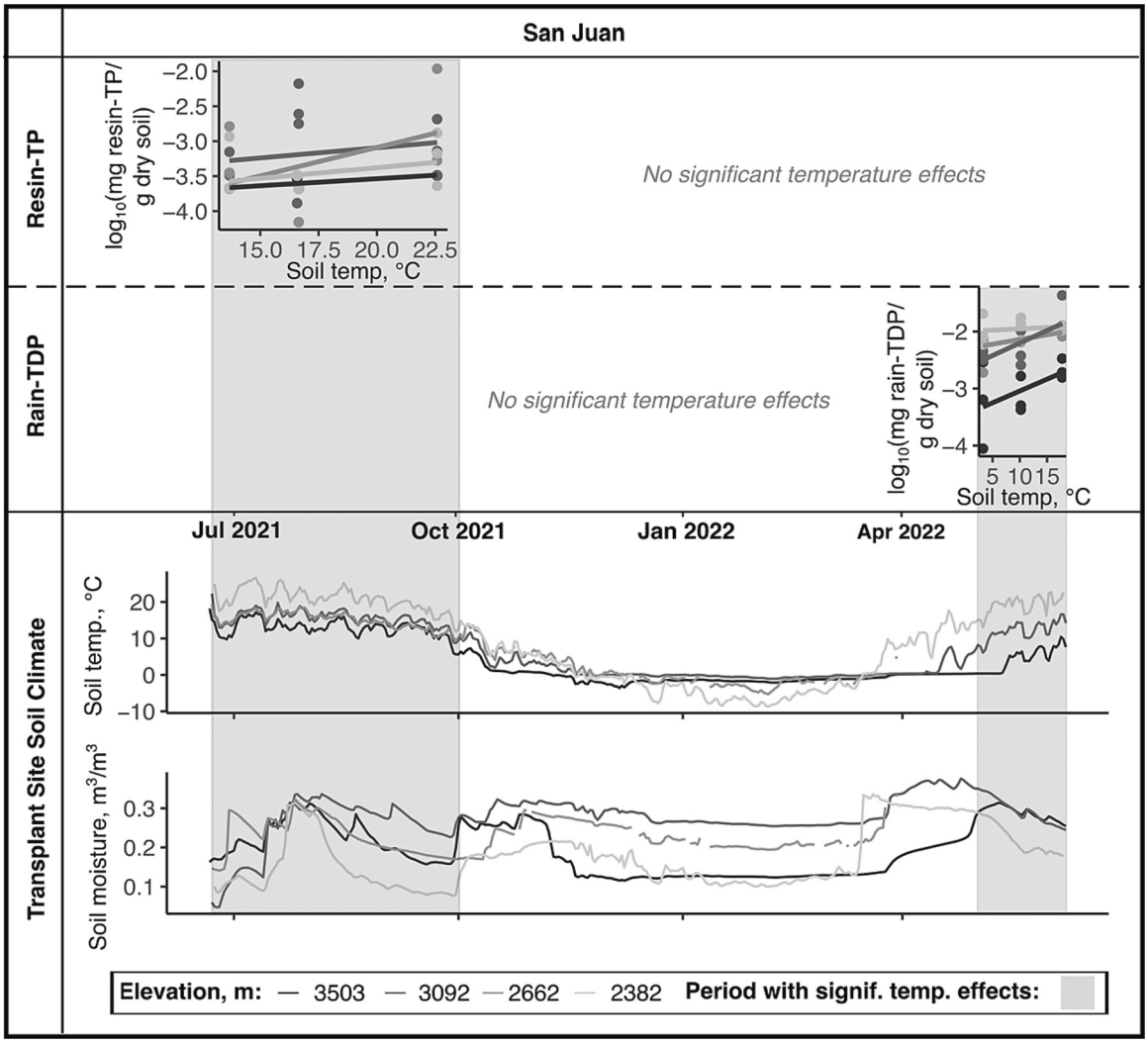

Fig. 3. Stacked scatterplots and line graphs showing significant relationships between temperature and resin total phosphorus (Resin-TP) and rain-soluble total dissolved phosphorus (Rain-TP) in the San Juan mountains. The width of these scatterplots corresponds with the time period during which the observed temperature effect occurred (indicated by grey shaded regions). Transplant site soil temperature and moisture line graphs for each range are displayed below scatterplots. Reported *P*-values are the result of linear mixed modeling and were estimated using the Satterthwaite method (Satterthwaite, 1941).

order of magnitude larger (0.019 mg P/g dry soil) than soils with pH < 7 and bulk density ≥ 1.2 g/cm^2 (0.0011 mg P/g dry soil).

4. Discussion

The results presented above present three primary takeaways with respect to our hypothesis that higher soil temperatures would increase P release by accelerating decomposition and weathering rates: (1) Higher soil temperatures can increase P mobilization in a field setting (transplant experiments), (2) low soil moisture can limit soil microbial activity and negate the effects of temperature on P release, and (3) soil properties strongly influence soil rain-soluble P concentrations and, by extension, the magnitude of any warming-driven P release. Because soil moisture is strongly influenced by temperature in mountain environments, this interplay between soil temperature and moisture effects suggests that there could be a stabilizing interaction that limits mountain soil P release as temperature increases. In combination, these three findings suggest that the relative magnitude of any warming-induced increases in P release will vary substantially among mountain ranges with different soil types. In the following sections, we discuss what these results mean for our hypothesis that higher soil temperatures are increasing P concentrations in mountain lakes and streams and compare these findings with previous research.

4.1. Transplant experiments: higher temperatures can increase P mobilization

Results from our transplant experiments show that higher temperatures can increase soil P mobilization in a field setting (Figs. 3, 4), which suggests that higher soil temperatures could drive significant P loading in mountain watersheds under some circumstances. In both study mountain ranges, soil temperature and moisture effects were confounded to some degree. During periods with significant positive soil temperature effects, there were also generally significant negative soil moisture effects (Tables 1, 2). Strong negative correlations between soil temperature and soil moisture in both ranges make it statistically impossible to determine which variable is driving the observed changes in P. However, previous studies have shown that low soil moisture generally limits microbial activity and nutrient mobilization (e.g. Davidson et al., 1998), so it is more likely that the observed increases in P are driven by high soil temperature rather than by low soil moisture. Assuming that this is the case, our results showed that rain-soluble P increased by up to 0.04 mg P/g dry soil in cores transplanted to warmer sites relative to disturbance control cores from the same source site.

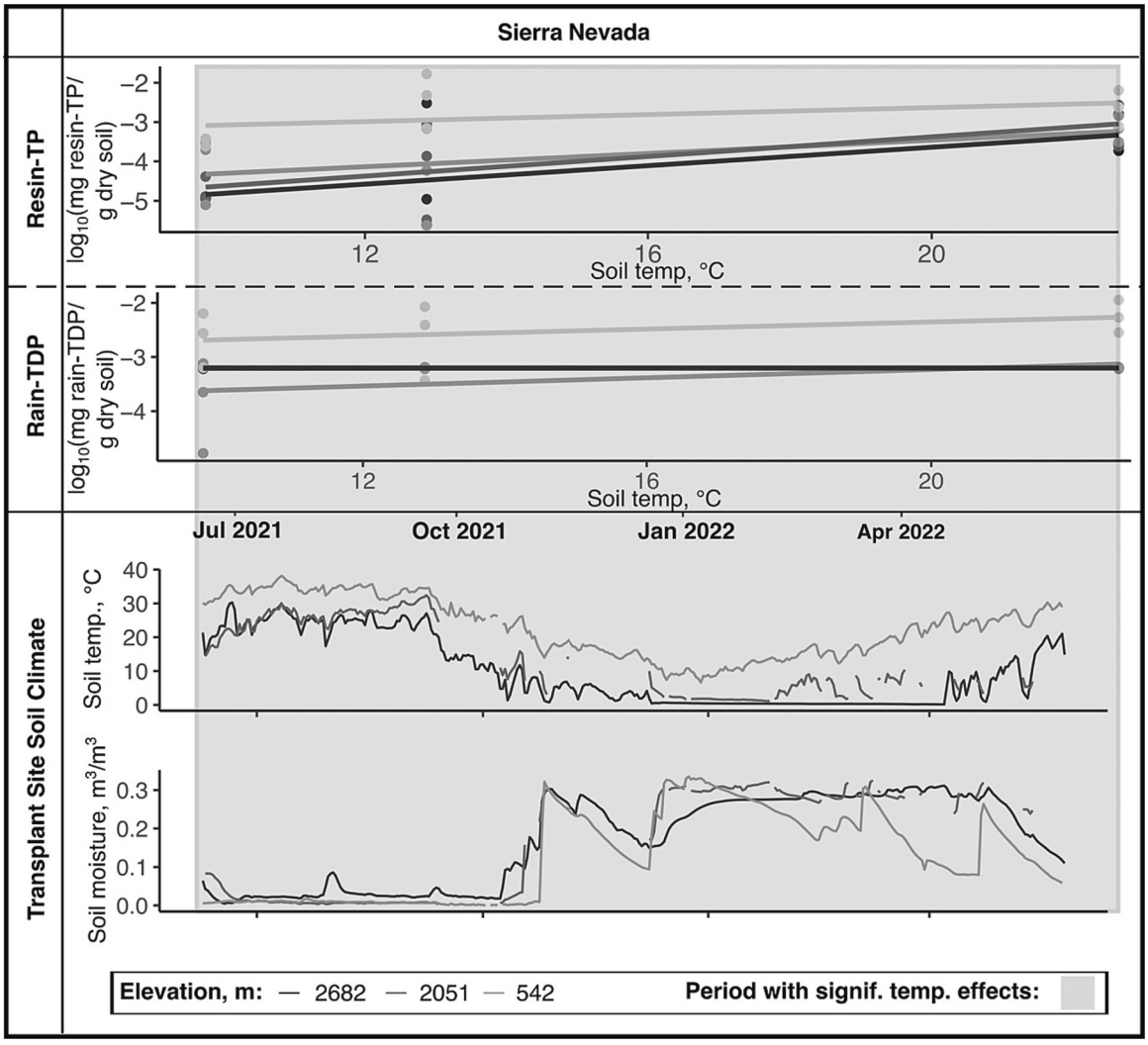

Fig. 4. Stacked scatterplots and line graphs showing significant ($P < 0.05$) and marginally significant ($P < 0.1$) relationships between temperature and resin total phosphorus (Resin-TP) and rain-soluble total dissolved phosphorus (Rain-TP) Sierra Nevada mountains. The width of these scatterplots corresponds with the time period during which the observed temperature effect occurred (indicated by grey shaded regions). Transplant site soil temperature and moisture line graphs for each range are displayed below scatterplots. Reported *P*-values are the result of linear mixed modeling and were estimated using the Satterthwaite method (Satterthwaite, 1941).

Table 2
Descriptive statistics for linear mixed models testing soil climate effects on rain-soluble total dissolved phosphorus (rain-TP), phosphatase enzyme (ptase) activity, and resin-bead total phosphorus (resin-TP) in the Sierra Nevada mountains. Significant predictor variables included annual average soil temperature (annual temp.) and soil moisture (annual moisture).

Rain-TP					
Model	AIC	β	df_{Sat}	T	P_{Sat}
log_{10}(rain TP) ~ Annual Temp.	42.68	0.02	30.05	1.68	0.10
log_{10}(rain TP) ~ Annual Moisture	42.68	−7.71	30.04	−1.79	0.08

Ptase activity
No significant predictors

Resin-TP					
Model	AIC	β	df_{Sat}	T	P_{Sat}
log_{10}(resin TP) ~ Annual Temp.	95.23	0.09	30.09	3.69	<0.01
log_{10}(resin TP) ~ Annual Moisture	94.70	−35.53	30.08	−3.79	<0.01

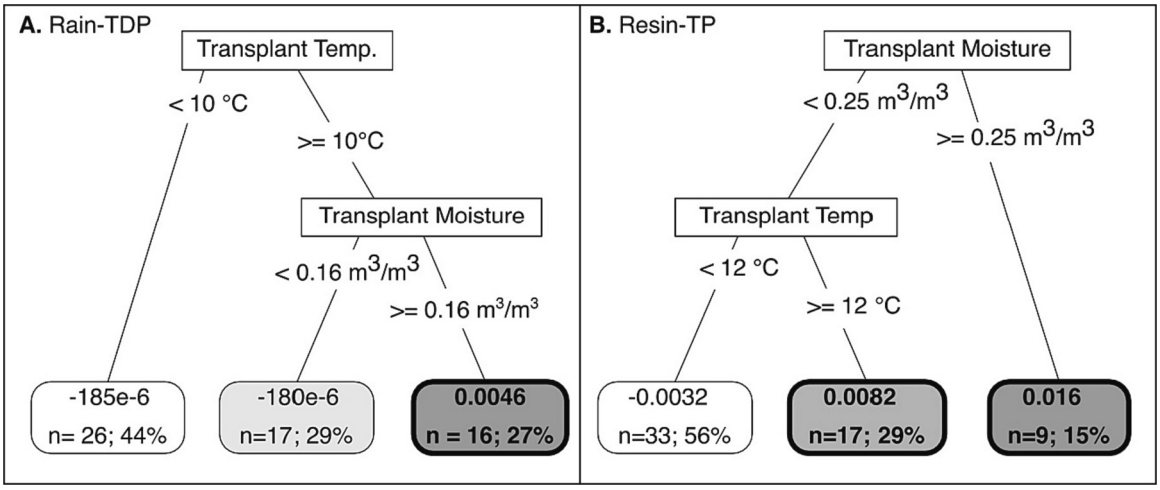

Fig. 5. Regression tree models showing relationships between change in rain-TDP (left)/change in resin-TP (right) and transplant site soil temperature and moisture. Leaf nodes report the mean value of samples in that node along with the number (n) and percentage of samples grouped into that node. Nodes with bold outlines and text indicate cases in which either rain-TDP or resin-TP increased, while un-bolded nodes indicate cases in which rain-TDP or resin-TP decreased. Increases in rain-TDP occurred only when both transplant site soil temperature and moisture were elevated. Increases in resin-TP occurred either when soil moisture was elevated or when soil moisture was lower but soil temperatures were elevated.

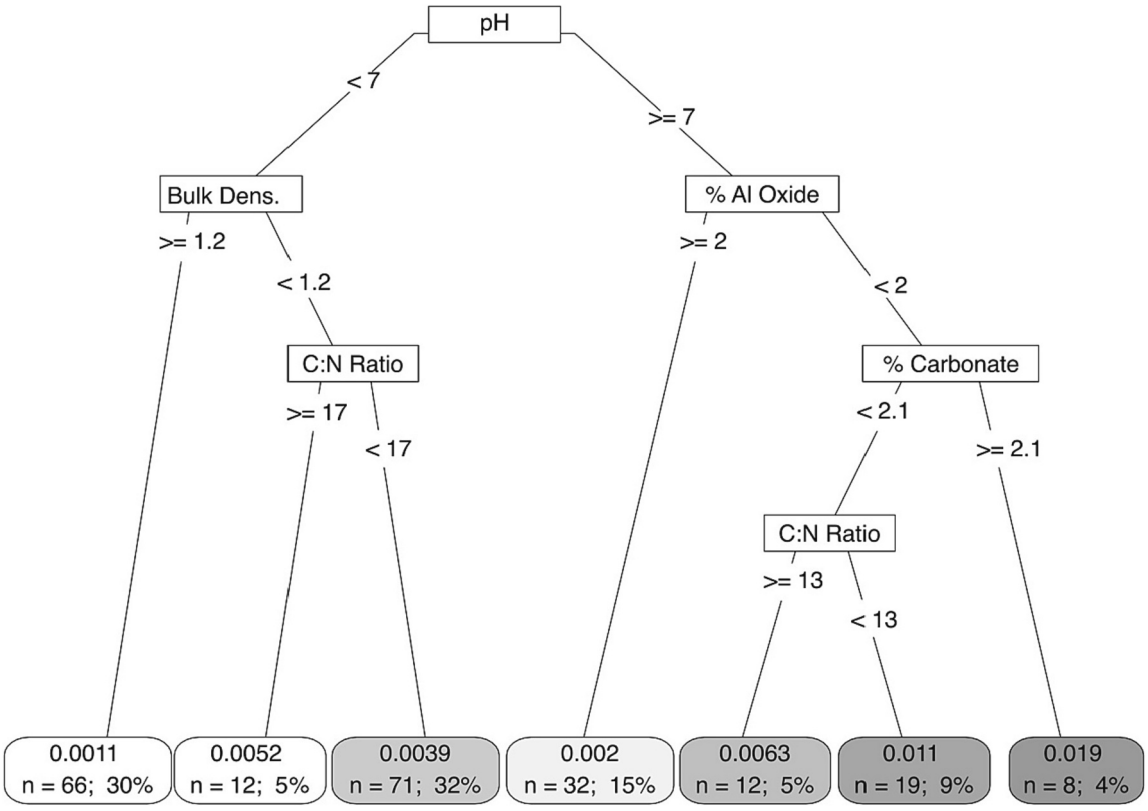

Fig. 6. Regression tree model showing the effects of various soil properties on rain-TDP concentrations across all study mountain ranges and experimental treatments. Leaf nodes report the mean value of samples in that group (top) along with the number (n) and percentage of samples falling into that group (bottom). The model suggests that soils with higher pH, lower aluminum (Al) oxide concentrations, and higher carbonate contents tend to have the highest rain-TDP concentrations.

Increases of this magnitude may appear relatively small, but when multiplied across entire mountain watersheds, they could result in substantial increases in mountain lake P inputs. For example, assuming a soil depth of 10 cm and using the mean bulk density (0.90 g/cm^3) and soil wetness (0.07 g/g) of cores that saw P increases of 0.04 mg P/g dry soil, increases of this magnitude would result in an increase in rain-soluble P of 3.1 g P/m^2.

Notably, these measurements estimate "net" soil P export rather than directly measuring SOM decomposition rates, so directly linking these findings to decomposition rates is challenging. For example, while temperature is generally expected to increase SOM decomposition rates, soil microbial growth and respiration also generally increase with higher temperature (Bååth, 2018). As a result, microbial P uptake may also increase with increasing temperature, potentially counteracting the

effects of increased decomposition rates on soil P export. Furthermore, as we sampled only very limited areas of the landscape, projecting our results onto entire mountain landscapes is difficult – some soils may be more or less susceptible to warming-driven P releases than the soils studied here, and estimating this variability is well beyond the scope of this study. With this context in mind, our results indicate that higher temperatures can increase soil P mineralization in excess of microbial P uptake and soil P sorption rates in the field for at least some parts of mountain landscapes. In total, these results support our hypothesis that higher soil temperatures could increase mountain soil P export and, by extension, P input to mountain lakes and streams. However, results from our incubation experiments add some nuance to this finding by showing that low soil moisture can limit soil microbial activity and negate the effects of temperature on soil P export.

4.2. Incubation experiments: soil moisture limits soil microbial activity

While our transplant experiments provided evidence that higher soil temperatures can increase P mobilization in mountain soils, our incubation experiments showed that soil moisture can mediate the temperature sensitivity of soil P mobilization by limiting microbial activity. We expected higher incubation temperatures to increase both soil respiration and soil P mobilization, but our results showed that temperature had no effect on either variable. The lack of a significant temperature effect could be explained by (A) the relatively small degree of warming employed in our experiments or (B) the short duration of incubation experiments relative to transplant experiments. If geochemical weathering was the primary driver of soil P release in the soils studied, it is possible that incubation experiments were simply too short to cause any measurable change in geochemical weathering-driven P release. However, Scholz and Brahney (2022) found significant temperature-driven increases in mountain soil P release using very similar incubation experiment methodology. They showed that soil P export increased significantly after just 10–14 days of warming with similar temperature differences between incubation treatments. This shows that (A) small changes in temperature can cause measurable increases in mountain soil P export and (B) the process driving these increases can be measurably accelerated in just 10–14 days, making a weathering an unlikely driver of the observed increases in P.

With this in mind, the most likely explanation for the difference between our results and the findings of previous incubation studies is differences in soil moisture conditions between our incubations and previous studies. Both Scholz and Brahney (2022) and Shaw and Cleveland (2020) raised soil moisture to field capacity prior to incubation, while we did not change soil moisture prior to incubation. As a result, our soils were much drier on average during the incubation treatments, and other evidence indicates that this low soil moisture may have limited the effects of temperature on soil P export. Our results showed that there was a strong positive correlation between high soil moisture and soil respiration in our experiments, indicating that soil microbial activity was limited by moisture rather than temperature in our experiments. This result is consistent with other studies that have shown that low soil moisture can limit both microbial respiration and soil nutrient production such that higher temperatures have no effect on either variable (e.g., Davidson et al., 1998; Allison and Treseder, 2008). This effect may explain why significant temperature effects were only observed during the summer and late spring in the San Juans, as soil moisture was relatively high during both periods (Fig. 3). It also suggests that the observed P increase in the Sierra Nevada occurred during the winter or spring, as soil moisture was very low during the summer (Fig. 4).

This interaction between soil moisture and temperature may act to limit the effects of increasing temperature on nutrient cycling in mountain soils. For much of the western United States, including mountainous regions, future warming is expected to be accompanied by drying (USGCRP, 2018), so it is possible that the limiting effect of low soil moisture may prevent higher soil temperatures from increasing P export from mountain soils into lakes and streams. Additionally, this relationship may explain the discrepancy between the results reported here and the findings of previous incubation studies that have found significant increases in soil P export and availability in response to elevated temperature (Shaw and Cleveland, 2020; Scholz and Brahney, 2022). Previous studies of temperature effects on soil P have adjusted soil moisture to relatively high, constant levels (e.g., field capacity) prior to incubation, eliminating the potential for low soil moisture to limit microbial activity and P export. Our findings suggest that this study design may result in an overestimate of warming effects on soil P mobilization.

4.3. Soil property analysis: soil properties control overall soil P pool sizes

Regression tree modeling showed that soils with neutral pH, low Al oxide concentration, and high carbonate content had an average rain-soluble P concentration order of magnitude larger (0.019 mg P/g dry soil) than more acidic soils with high bulk densities (0.0011 mg P/g dry soil). These soil properties have been linked with higher P availability (low bulk density, low Al oxide content, neutral soil pH; Kruse et al., 2015) and faster SOM decomposition (lower C:N ratios; Swift et al., 1979), so it is unsurprising that such soils would have larger labile soil P pools. Because the overall size of the labile soil P pool varies so widely between different soil types, the potential for warming-driven P release from these soils is also dramatically different. As an example of this effect, if both soil types described above underwent a 5 % increase in rain-soluble P export due to an increase in temperature, the total export from the higher P soil would increase by 0.001 mg P/g dry soil, while export from the low P soil would increase by just 5.5×10^{-5} mg P/g dry soil. This substantial difference in the overall size of the soluble P pool could mean that measurable increases in P mobilization in response to warming would occur only in watersheds with high-P soils. This pattern could explain why Scholz and Brahney (2022) only observed significant P increases in soils from mountain ranges with higher bedrock P concentrations. While the specific combinations of soil properties discussed above is specific to our dataset, our results highlight the importance of considering local soil properties in predicting the spatial distribution of warming-induced soil P increases.

4.4. Future patterns of warming-induced P flux

In total, our findings suggest that the degree to which higher soil temperatures increase P delivery to mountain lakes will depend on soil moisture conditions and watershed soil properties. Specifically, our results indicate that mountain landscapes that (1) experience warming concurrent with elevated soil moisture and (2) have soils rich in P are the most likely to have significant increases in soil P mobilization. These criteria can be used as a general framework to predict which mountain watersheds may be most susceptible to significant increases in soil P mobilization as soil temperatures increase due to the warming climate.

Large-scale climate models can provide some insight into which mountain regions may experience such combined warming and wetting. Evidence suggests that temperatures are increasing more rapidly in mountain regions than in adjacent lowlands across the world (Pepin et al., 2015), but predictions of future precipitation patterns are more variable. In general, climate models predict that winter precipitation will increase while summer precipitation will decrease for most of the United States (USGCRP, 2018). Based on these predictions, our findings suggest that low soil moisture may prevent warming from increasing soil P mobilization during hotter, drier summers, but that concurrent warming and wetting during the winter months may drive significant increases in P-mobilization. This effect may be the most pronounced in higher-latitude mountain ranges, which are predicted to experience larger increases in both temperature and winter precipitation (USGCRP, 2018). Some studies have already found evidence of a warming-driven

increase in P leaching during the winter months (Kaštovská et al., 2022), and future changes in climate are likely to exacerbate this trend. One caveat to this prediction is that mean wettest day precipitation totals are projected to increase even in regions that see declines in annual average precipitation (IPCC, 2023). Previous incubation studies have found significant increases in soil P mobilization after only 12–14 days (Shaw and Cleveland, 2020; Scholz and Brahney, 2022), so it is possible that these short periods of elevated soil moisture following intense precipitation events may be sufficient to accelerate soil P mobilization.

In addition to climatic factors, our results also show that local soil properties exert a strong control on the overall size of the soluble soil P pool and, by extension, the overall amount of potential P mobilization that could occur. When combined with the climatic factors discussed above, our results indicate that mountain watersheds with high-P soils that experience combined warming and wetting will be the most susceptible to warming-driven increases in soil P export. Other factors including vegetation cover and topography are also likely to influence the extent to which warming and wetting affect soil P export. While estimating these effects is beyond the scope of this study, future research should test how these and other landscape variables change the reported relationships between soil moisture, soil temperature, and soil P export.

5. Conclusions

In this study, we tested whether environmentally relevant levels of soil warming increased mountain soil P production using a combination of lab and field experiments. Our results show that warming can increase soil P mobilization under field conditions, but that this effect can be limited by low soil moisture. Furthermore, we found that soil properties play a critical role in determining the size of the soluble soil P pool, which in turn determines the potential size of future increases in soil P mobilization. In combination, these findings indicate that mountain regions with higher-P soils and coincident increases in soil moisture and temperature may experience the largest increases in warming-induced soil P mobilization. In these regions, increased P loading has the potential to alter ecosystem structure and function in mountain lakes, with potentially serious implications for both local ecosystem integrity and downstream water quality.

CRediT authorship contribution statement

Gordon Gianniny: Writing – review & editing, Writing – original draft, Visualization, Software, Methodology, Investigation, Funding acquisition, Formal analysis, Data curation. **John M. Stark:** Writing – review & editing, Validation, Supervision, Resources, Conceptualization. **Benjamin W. Abbott:** Writing – review & editing, Resources, Investigation, Funding acquisition. **Raymond Lee:** Writing – review & editing, Resources, Investigation, Funding acquisition. **Janice Brahney:** Writing – review & editing, Supervision, Resources, Project administration, Methodology, Funding acquisition, Conceptualization.

Declaration of competing interest

The authors declare the following financial interests/personal relationships which may be considered as potential competing interests: Janice Brahney reports financial support was provided by Utah State University Agricultural Experiment Station. Gordon Gianniny reports financial support was provided by Geological Society of America. If there are other authors, they declare that they have no known competing financial interests or personal relationships that could have appeared to influence the work reported in this paper.

Data availability

Data will be made available on request.

Acknowledgements

This research was supported by the Utah Agricultural Experiment Station, Utah State University, and approved as journal paper number 9678. This study would not have been possible without the help of Lauren Jones, Jens Ammon, and Nate Omer in both the field and lab. We also appreciate the support of Sequoia National Park, Bureau of Land Management, and US Forest Service in facilitating sample collection. Finally, we would like to thank Susan Durham for providing guidance in developing our statistical analyses.

Appendix A. Supplementary data

Supplementary data to this article can be found online at https://doi.org/10.1016/j.scitotenv.2024.170958.

References

Allison, S.D., Treseder, K.K., 2008. Warming and drying suppress microbial activity and carbon cycling in boreal forest soils. Glob. Chang. Biol. 14, 2898–2909. https://doi.org/10.1111/j.1365-2486.2008.01716.x.

Arroyo, J.I., Díez, B., Kempes, C.P., et al., 2022. A general theory for temperature dependence in biology. Proc. Nat. Acad. Sci. 119, e2119872119 https://doi.org/10.1073/pnas.2119872119.

Bååth, E., 2018. Temperature sensitivity of soil microbial activity modeled by the square root equation as a unifying model to differentiate between direct temperature effects and microbial community adaptation. Glob. Chang. Biol. 24, 2850–2861. https://doi.org/10.1111/gcb.14285.

Bates, D., Mächler, M., Bolker, B., Walker, S., 2014. Fitting Linear Mixed-effects Models Using lme4.

Brahney, J., Ballantyne, A.P., Kociolek, P., et al., 2014. Dust mediated transfer of phosphorus to alpine lake ecosystems of the Wind River Range, Wyoming, USA. Biogeochemistry 120, 259–278. https://doi.org/10.1007/s10533-014-9994-x.

Brahney, J., Mahowald, N., Ward, D.S., et al., 2015. Is atmospheric phosphorus pollution altering global alpine Lake stoichiometry? Glob. Biogeochem. Cycles 29, 1369–1383. https://doi.org/10.1002/2015GB005137.

Brantley, S.L., Shaughnessy, A., Lebedeva, M.I., Balashov, V.N., 2023. How temperature-dependent silicate weathering acts as Earth's geological thermostat. Science 379, 382–389. https://doi.org/10.1126/science.add2922.

Camarero, L., Catalan, J., 2012. Atmospheric phosphorus deposition may cause lakes to revert from phosphorus limitation back to nitrogen limitation. Nat. Commun. 3, 1118. https://doi.org/10.1038/ncomms2125.

Soil sampling and methods of analysis. In: Carter, M.R., Gregorich, E.G. (Eds.), 2008. Canadian Society of Soil Science, 2nd ed. CRC Press, [Pinawa, Manitoba]: Boca Raton, FL.

Cataldo, D.A., Maroon, M., Schrader, L.E., Youngs, V.L., 1975. Rapid colorimetric determination of nitrate in plant tissue by nitration of salicylic acid. Commun. Soil Sci. Plant Anal. 6, 71–80. https://doi.org/10.1080/00103627509366547.

Conant, R.T., Ryan, M.G., Ågren, G.I., et al., 2011. Temperature and soil organic matter decomposition rates – synthesis of current knowledge and a way forward. Glob. Chang. Biol. 17, 3392–3404. https://doi.org/10.1111/j.1365-2486.2011.02496.x.

Davidson, E.A., Belk, E., Boone, R.D., 1998. Soil water content and temperature as independent or confounded factors controlling soil respiration in a temperate mixed hardwood forest. Glob. Chang. Biol. 4, 217–227. https://doi.org/10.1046/j.1365-2486.1998.00128.x.

Davidson, T.A., Sayer, C.D., Jeppesen, E., et al., 2023. Bimodality and alternative equilibria do not help explain long-term patterns in shallow lake chlorophyll-a. Nat. Commun. 14, 398. https://doi.org/10.1038/s41467-023-36043-9.

Goldman, C.R., 1988. Primary productivity, nutrients, and transparency during the early onset of eutrophication in ultra-oligotrophic Lake Tahoe, Califomia-Nevada1. Limnol. Oceanogr. 33, 1321–1333. https://doi.org/10.4319/lo.1988.33.6.1321.

Grover, B., Johnson, R., Tutu, H., 2016. Leachability of metals from gold tailings by rainwater: an experimental and geochemical modelling approach. Water SA 42, 38. https://doi.org/10.4314/wsa.v42i1.05.

IPCC, 2023. Climate Change 2022: Impacts, Adaptation, and Vulnerability. Intergovernmental Panel on Climate Change.

Kaštovská, E., Choma, M., Čapek, P., et al., 2022. Soil warming during winter period enhanced soil N and P availability and leaching in alpine grasslands: a transplant study. PLoS ONE 17, e0272143. https://doi.org/10.1371/journal.pone.0272143.

Koch, O., Tscherko, D., Kandeler, E., 2007. Temperature sensitivity of microbial respiration, nitrogen mineralization, and potential soil enzyme activities in organic alpine soils. Glob. Biogeochem. Cycles 21. https://doi.org/10.1029/2007GB002983.

Kopàček, J., Hejzlar, J., Vrba, J., Stuchlík, E., 2011. Phosphorus loading of mountain lakes: terrestrial export and atmospheric deposition. Limnol. Oceanogr. 56, 1343–1354. https://doi.org/10.4319/lo.2011.56.4.1343.

Kopáček, J., Kaňa, J., Bičárová, S., et al., 2019. Climate change accelerates recovery of the Tatra Mountain lakes from acidification and increases their nutrient and chlorophyll a concentrations. Aquat. Sci. 81, 70. https://doi.org/10.1007/s00027-019-0667-7.

Krebs, D.C.J., 2013. Chapter 8, Sampling designs: random sampling. In: Adaptive and Systematic Sampling, p. 56.

Kruse, J., Abraham, M., Amelung, W., et al., 2015. Innovative methods in soil phosphorus research: a review. J. Plant Nutr. Soil Sci. 178, 43–88.
Kuhn, M., 2015. caret: classification and regression training. In: Astrophys Source Code Libr ascl:1505.003.
Kuznetsova, A., Brockhoff, P.B., Christensen, R.H.B., 2017. lmerTest package: tests in linear mixed effects models. J. Stat. Softw. 82, 1–26. https://doi.org/10.18637/jss.v082.i13.
Link, S.O., Smith, J.L., Halvorson, J.J., Bolton, H., 2003. A reciprocal transplant experiment within a climatic gradient in a semiarid shrub-steppe ecosystem: effects on bunchgrass growth and reproduction, soil carbon, and soil nitrogen. Glob. Chang. Biol. 9, 1097–1105. https://doi.org/10.1046/j.1365-2486.2003.00647.x.
Morales-Baquero, R., Pulido-Villena, E., Reche, I., 2006. Atmospheric inputs of phosphorus and nitrogen to the southwest Mediterranean region: biogeochemical responses of high mountain lakes. Limnol. Oceanogr. 51, 830–837. https://doi.org/10.4319/lo.2006.51.2.0830.
Moser, K.A., Baron, J.S., Brahney, J., et al., 2019. Mountain lakes: eyes on global environmental change. Glob. Planet. Chang. 178, 77–95. https://doi.org/10.1016/j.gloplacha.2019.04.001.
Mu, C., Abbott, B.W., Norris, A.J., et al., 2020. The status and stability of permafrost carbon on the Tibetan Plateau. Earth Sci. Rev. 211, 103433 https://doi.org/10.1016/j.earscirev.2020.103433.
Murphy, J., Riley, J.P., 1962. A modified single solution method for the determination of phosphate in natural waters. Anal. Chim. Acta 27, 31–36. https://doi.org/10.1016/S0003-2670(00)88444-5.
Nelson, D.W., 1983. Determination of ammonium in KCl extracts of soils by the salicylate method. Commun. Soil Sci. Plant Anal. 14, 1051–1062. https://doi.org/10.1080/00103628309367431.
Noe, G.B., 2011. Measurement of net nitrogen and phosphorus mineralization in wetland soils using a modification of the resin-core technique. Soil Sci. Soc. Am. J. 75, 760–770. https://doi.org/10.2136/sssaj2010.0289.
Oleksy, I.A., Baron, J.S., Leavitt, P.R., Spaulding, S.A., 2020. Nutrients and warming interact to force mountain lakes into unprecedented ecological states. Proc. R. Soc. B Biol. Sci. 287, 20200304 https://doi.org/10.1098/rspb.2020.0304.
Olson, N.E., Boaggio, K.L., Rice, R.B., et al., 2023. Wildfires in the western United States are mobilizing PM2.5-associated nutrients and may be contributing to downwind cyanobacteria blooms. Environ. Sci. Process Impacts 25, 1049–1066. https://doi.org/10.1039/D3EM00042G.
Pepin, N., Bradley, R.S., Diaz, H.F., et al., 2015. Elevation-dependent warming in mountain regions of the world. Nat. Clim. Chang. 5, 424–430. https://doi.org/10.1038/nclimate2563.
Powers, R.F., 1990. Nitrogen mineralization along an altitudinal gradient: interactions of soil temperature, moisture, and substrate quality. For. Ecol. Manag. 30, 19–29. https://doi.org/10.1016/0378-1127(90)90123-S.
Qin, B., Gao, G., Zhu, G., et al., 2013. Lake eutrophication and its ecosystem response. Chin. Sci. Bull. 58, 961–970. https://doi.org/10.1007/s11434-012-5560-x.
R Core Team, 2022. R: A Language and Environment for Statistical Computing.
Satterthwaite, F.E., 1941. Synthesis of variance. Psychometrika 6, 309–316. https://doi.org/10.1007/BF02288586.
Schimel, J.P., Clein, J.S., 1996. Microbial response to freeze-thaw cycles in tundra and taiga soils. Soil Biol. Biochem. 28, 1061–1066. https://doi.org/10.1016/0038-0717(96)00083-1.
Scholz, J., Brahney, J., 2022. Evidence for multiple potential drivers of increased phosphorus in high-elevation lakes. Sci. Total Environ. 825, 153939 https://doi.org/10.1016/j.scitotenv.2022.153939.
Shaw, A.N., Cleveland, C.C., 2020. The effects of temperature on soil phosphorus availability and phosphatase enzyme activities: a cross-ecosystem study from the tropics to the Arctic. Biogeochemistry 151, 113–125. https://doi.org/10.1007/s10533-020-00710-6.
Stenberg, B., Johansson, M., Pell, M., et al., 1998. Microbial biomass and activities in soil as affected by frozen and cold storage. Soil Biol. Biochem. 30, 393–402. https://doi.org/10.1016/S0038-0717(97)00125-9.
Stoddard, J.L., Van Sickle, J., Herlihy, A.T., et al., 2016. Continental-scale increase in lake and stream phosphorus: are oligotrophic systems disappearing in the United States? Environ. Sci. Technol. 50, 3409–3415. https://doi.org/10.1021/acs.est.5b05950.
Swift, M.J., Heal, O.W., Anderson, J.M., Anderson, J.M., 1979. Decomposition in Terrestrial Ecosystems. University of California Press.
Tabatabai, Ma, 1994. Soil enzymes. In: Methods of Soil Analysis. John Wiley & Sons, Ltd, pp. 775–833.
Therneau, T., Atkinson, B., 2022. rpart: Recursive Partitioning and Regression Trees.
USGCRP, 2018. Fourth National Climate Assessment. U.S. Global Change Research Program, Washington, DC.
Wallenstein, M., Allison, S.D., Ernakovich, J., et al., 2010. Controls on the temperature sensitivity of soil enzymes: a key driver of in situ enzyme activity rates. In: Shukla, G., Varma, A. (Eds.), Soil Enzymology. Springer Berlin Heidelberg, Berlin, Heidelberg, pp. 245–258.
Waring, B., Hawkes, C.V., 2018. Ecological mechanisms underlying soil bacterial responses to rainfall along a steep natural precipitation gradient. FEMS Microbiol. Ecol. 94 https://doi.org/10.1093/femsec/fiy001.
Weintraub, M.N., 2011. Biological phosphorus cycling in arctic and alpine soils. In: Bünemann, E., Oberson, A., Frossard, E. (Eds.), Phosphorus in Action. Springer Berlin Heidelberg, Berlin, Heidelberg, pp. 295–316.